Non-fermi-liquid behavior in a disordered Kondo-alloy model

D. R. Grempel*
Département de Recherche Fondamentale sur la Matière Condensée, SPSMS, CEA-Grenoble, 38054 Grenoble Cedex 9, France

M. J. Rozenberg
Departamento de Física, Facultad de Ciencias Exactas y Naturales, Universidad de Buenos Aires, Ciudad Universitaria, (1428) Buenos Aires, Argentina

(Received 10 February 1999)

We study a mean-field model of a Kondo alloy using numerical techniques and analytic approximations. In this model, randomly distributed magnetic impurities interact with a band of conduction electrons and have a residual Ruderman-Kittel-Kasuya-Yosida coupling of strength J. This system has a quantum-critical point at $J=J_c\sim T_K^0$, the Kondo scale of the problem. The T dependence of the spin susceptibility near the quantum critical point is singular with $\chi(0)-\chi(T)\propto T^\gamma$ and noninteger γ. At J_c, $\gamma=3/4$. For $J\lesssim J_c$ there are two crossovers with decreasing T, first to $\gamma=3/2$ and then to $\gamma=2$, the Fermi-liquid value. The dissipative part of the time-dependent susceptibility $\chi''(\omega)\propto\omega$ as $\omega\to 0$ except at the quantum-critical point where we find $\chi''(\omega)\propto\sqrt{\omega}$. The characteristic spin-fluctuation energy vanishes at the quantum-critical point with $\omega_{sf}\sim(1-J/J_c)$ for $J\lesssim J_c$, and $\omega_{sf}\propto T^{3/2}$ at the critical coupling. [S0163-1829(99)03131-8]

I. INTRODUCTION

The understanding of metallic states that do not fit within the framework of Fermi-liquid theory is one of the important current challenges of condensed matter physics.[1] This issue is relevant to a large class of *f*-electron materials that present anomalies in their thermodynamic and transport properties at low temperature.[2] Two important features characterize the physics of these systems. One, is the interaction of the conduction electrons with localized magnetic moments *via* the Kondo coupling. The other, is the inevitable presence of disorder due to the alloying process. Several models in which non-Fermi-liquid (NFL) behavior arises as a consequence of the interplay between disorder and magnetic interactions have been proposed in the literature. In the Kondo-disorder model of Miranda *et al.*,[3] randomness in the local hybridization matrix element between localized and itinerant electrons is thought to be at the origin of NFL behavior. In this theory, the disorder generates a broad distribution of Kondo temperatures whose tail extends down to $T_K=0$. Therefore, a finite fraction of the localized spins remain unquenched at all temperatures and gives rise to singularities in the thermodynamic and transport properties.

In the metallic spin-glass model,[4–6] the focus is on the consequences of randomness in the Ruderman-Kittel-Kasuya-Yosida (RKKY) intersite couplings. This type of disorder is modeled by including a spin-glass-like exchange term in the Hamiltonian. The system has a quantum phase transition when the strength of the magnetic interaction J becomes comparable to the Kondo temperature of the underlying Kondo lattice, $T_K^{(0)}$. Beyond this point, the ground state is no longer a nonmagnetic metal but it exhibits long-range spin-glass order. NFL behavior results from the power-law behavior found in the neighborhood of the quantum-critical point, a scenario that is similar to that proposed to explain NFL behavior in systems close to ferro- or antiferromagnetic instabilities.[7]

In this paper, we study a mean-field Kondo-alloy model recently proposed and discussed by Sengupta and Georges.[5] In their paper, these authors did not solve the original Hamiltonian but a simpler solvable quantum-rotor problem[8] that was assumed to exhibit the same low-frequency behavior. Here, we solve numerically the Kondo-alloy model using classical and quantum Monte Carlo techniques. We find a quantum phase transition at $J=J_c\approx 1.15\ T_K^0$ where the zero-temperature spin-glass susceptibility of the system diverges. At the critical coupling, the T dependence of the uniform magnetic susceptibility is singular with $\chi(0)-\chi(T)\sim T^{3/4}$. This anomalous T dependence is also found above the crossover line $T/J_c\sim(1-J/J_c)^{2/3}$. Below this line, we still find unconventional behavior but the exponent is different, $\chi(0)-\chi(T)\sim T^{3/2}$. For $J\neq J_c$, the normal behavior, $\delta\chi\sim T^2$, is recovered at low enough temperature. The numerical results for the frequency dependence of the susceptibility are very well described over a wide range of temperature and frequencies by a simple approximate expression that we derive from the original model in the strong-coupling limit. The strong coupling solution reduces to that of the simplified model of Sengupta and Georges[5] in the $\omega\to 0$ limit. The spin-fluctuation spectrum is Fermi-liquid-like for $\omega\to 0$ everywhere except at $J=J_c$. We find $\chi''(\omega)\propto\omega$ for $\omega\lesssim\omega_{sf}$ where the spin-fluctuation frequency $\omega_{sf}\propto(1-J/J_c)$ for $J\lesssim J_c$ and $\omega_{sf}\propto T^{3/2}$ at the critical coupling. At the quantum-critical point, $\chi''(\omega)\propto\sqrt{\omega}$. This implies a slow decay of the spin-spin correlation function, $\langle S_z(t)S_z(0)\rangle\sim t^{-3/2}$, that anticipates the appearance of long-range order in the system.

The paper is organized as follows: In Sec. II, we introduce the model Hamiltonian and use it to derive an effective local action for the spin degrees of freedom. In Sec. III, we discuss two equivalent formulations of the effective model that are well suited for a numerical investigation of the problem. These are based on the formal equivalence between the Kondo-alloy problem and two other models. The first one is a classical one-dimensional Ising chain with short- and long-

range ferromagnetic interactions, and may be solved by classical Monte Carlo simulation. The second model system describes a single $S=1/2$ quantum spin evolving in the presence of two magnetic fields, one that is time dependent and random in the longitudinal direction, and another that is static and fixed in the transverse direction. This problem may be solved using a quantum Monte Carlo algorithm. The results of the simulations are presented in Sec. IV where we also derive a simple analytical approximation that allows for a transparent interpretation of the data. This is followed by a comparison of our results to those obtained by other authors.

II. THE MODEL

In a disordered Kondo alloy, randomly distributed spins interact with a band of conduction electrons through a local Kondo coupling. There is also a residual RKKY exchange interaction between the spins, which is random because of the disorder in their positions. Many of the systems studied experimentally exhibit uniaxial anisotropy as a result of strong crystal-field and spin-orbit effects. Therefore, to a first approximation, only the coupling between the components of the localized spins along the easy-axis needs to be considered. The simplest model with these characteristics is a Kondo-lattice model with an additional Ising-like random exchange term. The Hamiltonian of the model is

$$H=-\sum_{i,j,\sigma} t_{ij}c^{+}_{i\sigma}c_{j\sigma}+J^{K}_{||}\sum_{i} S^{z}_{i}s^{z}_{i}+\frac{J^{K}_{\perp}}{2}\sum_{i}(S^{+}_{i}s^{-}_{i}+\text{H.c.}) -\frac{1}{2}\sum_{i,j} J_{ij}S^{z}_{i}S^{z}_{j}. \tag{1}$$

Here, $\vec{S}_i$ is a localized spin operator at the ith site of a lattice of size N. The creation and destruction operators for the conduction electrons are $c^{+}_{i\sigma}$ and $c_{i\sigma}$ and $\vec{s}_i=1/2\Sigma_{\alpha,\beta}c^{+}_{i\alpha}\vec{\sigma}_{\alpha,\beta}c_{i\beta}$ is the local electronic spin density. The nearest-neighbor electron hopping integral is $t_{ij}=t/\sqrt{z}$ where z is the connectivity of the lattice, and $J^{K}_{||}$ and $J^{K}_{\perp}$ are the longitudinal and transverse Kondo couplings, respectively. The nearest-neighbor couplings between the spins, J_{ij}, are quenched random variables for which we assume for simplicity a Gaussian probability distribution with zero mean and variance $\langle J^{2}_{ij}\rangle=J^{2}/z$. The z-dependent normalization of the off-diagonal couplings t_{ij} and J_{ij} has been chosen such that the results in the $z\to\infty$ limit to be considered below are finite.[9]

The last term on the right-hand side of Eq. (1) is the well-known Sherrington Kirkpatrick model[10] that has a phase transition to a spin-glass state at $T^{0}_{g}\propto J$. The local Kondo coupling favors screening of the localized spins by the conduction electrons below a characteristic temperature T^{0}_{K}. As a consequence of the competition between these two terms, a spin-glass ground state is only possible for $J\geq J_c\sim T^{0}_{K}$. Therefore, $T_g\to 0$ as $J\to J_c$ from above and the system remains paramagnetic down to zero temperature for $J<J_c$. The point $T=0$, $J=J_c$ where the nature of the ground state of the system changes defines the quantum-critical point.[7,11]

We investigate the properties of model (1) near the quantum-critical point in the framework of a dynamical mean-field theory.[12] In this approach, exact in the limit of infinite lattice connectivity, the degrees of freedom on any particular lattice site are isolated and treated exactly, while the rest of the system is replaced by an effective medium to which the chosen site is coupled. The properties of the effective medium are determined self-consistently from the solution of the single-site problem. In the limit $z\to\infty$, the configurational average over the random couplings can be performed explicitly[13] and the intersite terms in Eq. (1) can be eliminated.[12] This reduces the problem to a magnetic impurity embedded in an electronic bath and subject to a dynamic magnetic selfinteraction.[12,13] Ignoring for the moment the anisotropy of the Kondo coupling in order to simplify the notation, the effective action of the single-site problem in the paramagnetic phase may be written as[5]

$$\mathcal{S}_{\text{loc}}=-\int_0^\beta\int_0^\beta d\tau d\tau' c^{+}_{\sigma}(\tau)\mathcal{G}_0^{-1}(\tau-\tau')c_{\sigma}(\tau') +J_K\int_0^\beta d\tau\vec{S}(\tau)\cdot\vec{s}(\tau)-\frac{J^2}{2}\int_0^\beta\int_0^\beta d\tau d\tau' S_z(\tau) \times\chi(\tau-\tau')S_z(\tau'). \tag{2}$$

The functions $\chi(\tau)$ and $\mathcal{G}_0(\tau)$, *a priori* unknown, are determined by the feedback effects of the coupling of the impurity site to rest of the system through a set of self-consistency conditions. Their precise form depends upon the shape of the noninteracting electronic density of states $\mathcal{N}(\epsilon)$ of the lattice.[12] In the case of a semicircular density of states, the self-consistency equations acquire a particularly simple form. We have

$$\chi(\tau)=\langle\mathcal{T}[S_z(\tau)S_z(0)]\rangle_{\mathcal{S}_{\text{loc}}}, \tag{3}$$

for the magnetic degrees of freedom, and

$$\mathcal{G}_0^{-1}(\tau-\tau')=\left(-\frac{\partial}{\partial\tau}+\mu\right)\delta(\tau-\tau')-t^2\mathcal{G}(\tau-\tau') \tag{4}$$

for the electronic degrees of freedom. In the above equations, $\mathcal{T}$ is the time-ordering operator along the imaginary-time axis $0\leq\tau\leq\beta$, μ is the chemical potential and

$$\mathcal{G}(\tau)=-\langle\mathcal{T}[c(\tau)c^{+}(0)]\rangle_{\mathcal{S}_{\text{loc}}}. \tag{5}$$

It follows that $\mathcal{G}$ and χ are, respectively, the exact local electronic Green function and the imaginary-time-dependent spin susceptibility. For general $\mathcal{N}(\epsilon)$, Eq. (4) is replaced by a more complicated implicit condition.[14]

The solution of this set of coupled self-consistent equations is still a very difficult task. It may be argued, however, that knowledge of the exact bath Green function is not essential for the understanding of the low-frequency spin dynamics of the model. This follows from a perturbative argument[5] that establishes that the long-time behavior of the exact bath Green function is qualitatively the same as that of a bath of noninteracting electrons, i.e., $\mathcal{G}_0(\tau)\sim 1/\tau$. But the form of the low-energy effective action for the localized spins is determined precisely by the asymptotic behavior of the electronic Green function. Therefore, if we ignore Eq. (4) and fix $\mathcal{G}_0(i\omega_n)=\int_{-\infty}^{\infty}d\epsilon\mathcal{N}_0(\epsilon)/(i\omega_n+\mu-\epsilon)$ where $\mathcal{N}_0(\epsilon)$

is the unrenormalized density of states, we will still get a qualitatively correct description of the low-frequency spin dynamics of the model.

Further progress can be made by performing a Hubbard-Stratonovich transformation that decouples the last term in Eq. (2). Introducing a set of time-dependent random fields $\eta(\tau)$ that couple to the spin operators,[15] the partition function of the problem may be rewritten as

$$Z=\int \mathcal{D}\eta(\tau)\exp\left[-\frac{1}{2}\int_0^\beta\int_0^\beta d\tau d\tau'\,\eta(\tau)\times\chi^{-1}(\tau-\tau')\,\eta(\tau')\right]Z_K[\eta], \tag{6}$$

where

$$Z_K[\eta]=\int \mathcal{D}c(\tau)\mathcal{D}c^+(\tau)\,\mathrm{Tr}_{S_z}\,(\mathcal{T}\exp-\mathcal{S}_K), \tag{7}$$

and

$$\mathcal{S}_K=-\int_0^\beta\int_0^\beta d\tau d\tau' c_\sigma^+(\tau)\mathcal{G}_0^{-1}(\tau-\tau')c_\sigma(\tau') + J_K\int_0^\beta d\tau\vec{S}(\tau)\cdot\vec{s}(\tau)-J\int_0^\beta d\tau S_z(\tau)\,\eta(\tau). \tag{8}$$

Equation (8) is the action of a single Kondo impurity in a time-dependent magnetic field $J\eta(\tau)$ in the z direction. Within dynamic mean-field theory the partition function of the Kondo alloy is thus given by the average over all the realizations of the random field of the partition function of the modified Kondo problem of Eq. (8).

Equations (6)–(8) subject to condition (3) define the mean-field model of the Kondo alloy. In the next section we shall show that this model may be cast in two different forms both of which are well suited for setting up schemes for the numerical solution of the problem.

III. METHOD

A. Formulation of the problem

As we are only interested in the spin dynamics of the system, the electronic degrees of freedom in Eq. (6) may be integrated out. In the case of the single-impurity Kondo model this leads to the well known Coulomb gas representation[16] of the partition function of the problem. The same is true for the generalized problem of Eq. (8) as the additional random term commutes with the longitudinal part of the Kondo coupling. The Anderson-Yuval technique[16] may therefore be applied to Eq. (7). After averaging the resulting expression over the distribution of random fields, Eq. (6) may be rewritten as

$$Z_{CG}=\sum_{n=0}^{\infty}\int_0^\beta d\tau_1\int_0^{\tau_1-\tau_0}d\tau_2\ldots\int_0^{\tau_{2n-1}-\tau_0}\times d\tau_{2n}\left(\frac{J_\perp^K}{2}\right)^{2n}\exp\left[\sum_{i<j}(-1)^{i+j}V(\tau_i-\tau_j)\right], \tag{9}$$

where

$$\frac{\partial^2 V(\tau)}{\partial\tau^2}=2\alpha\left(\frac{\pi}{\beta}\right)^2\sin^{-2}\frac{\pi\tau}{\beta}+J^2\chi(\tau), \tag{10}$$

and τ_0 is a short time cutoff of the order of the inverse bandwidth of the electron bath. The coupling constant $\alpha=(1+2\delta/\pi)^2$ where $\delta=-\tan^{-1}(\pi\tau_0 J_{||}^K/4)$ is the phase shift for scattering of electrons from a local potential $J_{||}^K/4$.

In Eq. (9), τ_i, $i=1,\ldots,2n$ are the positions on the time axis of successive spin-flips generated by the transverse part of the Kondo coupling and the function $V(\tau)$ represents the interaction between pairs of spin-flips. The first term on the righthand side of Eq. (10) is familiar from the work on the Kondo model.[16] It arises from the singular response of the conduction electron bath to a spin flip on the impurity site. The second term is characteristic of the alloy model and represents the reaction of the rest of the spins to the local perturbation. It is interesting to notice that the partition function of a recently studied extended two-band Hubbard model[17] can be cast in a form equivalent to Eq. (9).

Equation (9) is not yet in a form suitable for computation of the magnetic correlation function. We shall next establish a formal equivalence between Z_{CG} and the average partition function of a single quantum $S=1/2$ spin in the presence of a random Gaussian time-dependent longitudinal field $\xi(\tau)$ and a static transverse field Γ, a problem that can be solved numerically using the quantum Monte Carlo method of Refs. 15 and 18. The partition function of the quantum spin problem Z_{QS} is

$$Z_{QS}=\int \mathcal{D}\xi\,\exp\left[-\frac{1}{2}\int_0^\beta\int_0^\beta d\tau d\tau'\,\xi(\tau)Q^{-1}(\tau,\tau')\xi(\tau')\right]\times\mathrm{Tr}_{S_z}\,\mathcal{T}\exp\left[\int_0^\beta d\tau[\xi(\tau)S_z(\tau)+\Gamma S_x(\tau)]\right], \tag{11}$$

where $Q(\tau)$ is the correlation function of the random component of the magnetic field.

To demonstrate the equivalence of Eqs. (9) and (11), we first perform a Trotter decomposition of the time-ordered exponential in Eq. (11),

$$\mathcal{T}\exp\left[\int_0^\beta d\tau\vec{h}(\tau)\cdot\vec{S}(\tau)\right]\sim\prod_{k=1}^{M}\exp[\Delta\tau\vec{h}(\tau_k)\cdot\vec{S}], \tag{12}$$

where $\Delta\tau=\beta/M$. We next introduce a complete set of intermediate states $|\sigma_k\rangle\langle\sigma_k|$ at each imaginary time slice τ_k. The matrix elements in the Trotter expansion may be evaluated using the expression

$$\langle\sigma|\exp\{\Delta\tau[\xi(\tau)S_z(\tau)+\Gamma S_x(\tau)]\}|\sigma'\rangle \approx e^{\Delta\tau\xi(\tau)\sigma}\left[\delta_{\sigma\sigma'}+\delta_{\sigma\bar{\sigma}'}\frac{\Gamma\Delta\tau}{2}+\mathcal{O}(\Delta\tau^2)\right], \tag{13}$$

valid in the limit $\Delta\tau\to 0$. After averaging over the field $\xi(\tau)$ and taking the limit $M\to\infty$, the partition function of the model may be expressed as a sum of contributions of individual ''spin histories,'' each of these being one of the possible sequences of the eigenvalues $\sigma(\tau)=\pm 1/2$ of the intermediate states. We find

$$Z_{\rm QS}=\sum_{n=0}^{\infty}\int \mathcal{D}\sigma^{(n)}\exp\left[\frac{1}{2}\int_0^\beta\int_0^\beta d\tau d\tau'\,\sigma^{(n)}(\tau)\times Q(\tau-\tau')\sigma^{(n)}(\tau')+n\ln\Gamma\right], \tag{14}$$

where $\sigma^{(n)}(\tau)$ is a spin history with n spin flips in the interval $0\leqslant\tau\leqslant\beta$ and the integration is over their positions. Equation (9) follows from Eq. (14) by integrating twice by parts the first term in the exponential, provided that we choose $\Gamma=J_\perp^K$ and that we identify $Q(\tau)$ with the righthand side of Eq. (10). The original problem has thus been reduced to the evaluation of the partition function of Eq. (11) subject to the condition (3).

An alternative numerical method may be formulated by taking advantage of the asymptotic equivalence[19,20] between the Coulomb gas representation (9) of the Kondo problem and the partition function of a *classical* one-dimensional Ising spin chain with nearest-neighbor and long-range interactions. This problem may be solved numerically using standard classical Monte Carlo techniques as has been recently done for the single-impurity anisotropic Kondo model in Ref. 20. It may be shown by a straightforward generalization of the methods of Ref. 19 that the Ising-chain model relevant for our problem is

$$Z_{\rm I}=\sum_{\{S_i\}}\exp\left[\sum_{i\leqslant L}K_{\rm NN}S_iS_{i+1}+\sum_{i<j\leqslant L}K_{LR}(i-j)S_iS_j\right], \tag{15}$$

where the $S_i=\pm1$ are Ising variables and the number of sites in the chain is $L=\beta/\tau_0$. The spin-spin interaction consists of a short-range part, $K_{NN}\approx-1/2\ln(J_K\tau_0/2)$, and a long-range part given by

$$K_{LR}(i-j)=\frac{1}{4}\left\{\frac{2\alpha(\pi/N)^2}{\sin^2[\pi(j-1)/N]}+J^2\tau_0^2\chi(\tau_0|i-j|)\right\}. \tag{16}$$

It is worth noticing that, while both of these approaches can be used to solve the present strongly anisotropic Kondo-alloy model, only the first one can be generalized to the case of a non-Ising spin-spin interaction.

B. Numerical methods

We have simulated the mean-field Kondo-alloy model using the two formulations described in the previous section as each has its own advantages and drawbacks. In particular, while the systematic error introduced by the discretization of the imaginary time is larger for the quantum simulations, statistical fluctuations are far more important in the classical case. We have empirically found that the latter method is more accurate for the computation of the static susceptibility at low temperatures whereas the former one gives better results for the overall frequency dependence of the spin correlation function.

The numerical procedure used to solve the self-consistent problem is as follows: (i) an approximation to $\chi(\tau)$ is used as input in either Eqs. (10) or (16). (ii) the spin-spin correlation function is obtained from a Monte Carlo simulation (see below). (iii) a new $\chi(\tau)$ is computed from condition (3) and used as a new input in step (i). This procedure is iterated until successive values of the correlation function differ by less than a fixed tolerance level (see below). This takes from four to fifteen iterations depending on the temperature and the values of the parameters.

The simulations of the classical problem defined by Eq. (15) have been done using a standard Monte Carlo heat-bath algorithm for Ising chains of up to 256 sites. The quantum problem of Eq. (11) has been simulated as follows. The imaginary-time axis is discretized in slices of width $\Delta\tau=\beta/M$ and the time-ordered exponential appearing in Eq. (11) is approximated by a Trotter product of M factors. The statistical weight of a given configuration $\{\xi(\tau)\}$ is thus expressed in terms of the trace of a product of 2×2 random matrices. The corresponding contribution to the spin correlation function $\chi(\tau,\tau')$ is computed by inserting two additional σ_z Pauli matrices at the appropriate places in the matrix product. It is important to choose the parameter M appropriately. If M is too small, the systematic error introduced by the Trotter approximation is large. If M is too large, however, the algorithm is prone to numerical instability. We found that the choice $\beta\leqslant0.25M\tau_0$ with $M\leqslant128$ is a satisfactory compromise. This sets a lower limit to the temperatures that we can simulate, $\tau_0T_{\rm min}\approx0.03$. The simulation is most conveniently done in the space of the Masubara-frequency components of the field, $\xi(\omega_n)=\int_0^\beta d\tau\xi(\tau)\exp(-i\omega_n\tau)$.[15] These are finite in number as a consequence of the discretization of time: $\omega_n=2\pi nT$ with $n=0,\ldots,M-1$. In an elemental Monte Carlo move, a change of the complex field $\xi(\omega_n)$ for a single frequency is attempted. A full Monte Carlo step is complete when elemental changes have been attempted for all the Matsubara frequencies.

The accuracy of the numerical calculations presented below is determined by two factors, namely, the statistical error of the Monte Carlo calculation and the stopping criterion used in the enforcement the self-consistency condition. A typical quantum Monte Carlo run consisted of 4×10^5 Monte Carlo steps per time slice. This corresponds to an absolute error of the order of 2×10^{-3} in $\chi(\tau)$. As we mentioned above, the simulations based on Eq. (15) are noisier than those based on Eq. (11), which requires an order of magnitude more MC steps to reach the same level of accuracy. The self-consistency loop was stopped when two successive values of the static local susceptibility differed by less than 0.5%, which is about twice the size of the statistical error. On the basis of these figures, we estimate that our final results for χ_T are accurate to within 1%.

IV. RESULTS

We have simulated the mean-field Kondo alloy model for fixed values of the Kondo couplings and several values of J for $T\geqslant0.05\ T_K^0$ where T_K^0 is the single-site Kondo temperature (see below). The first step in the calculation is the choice of the parameters α, $J_\perp^K$ and τ_0 that define the underlying single-impurity Kondo problem [cf. Eq. (9)]. As the low-temperature properties of all antiferromagnetic Kondo models are described by the same fixed point, we are free to choose these parameters using criteria of numerical conve-

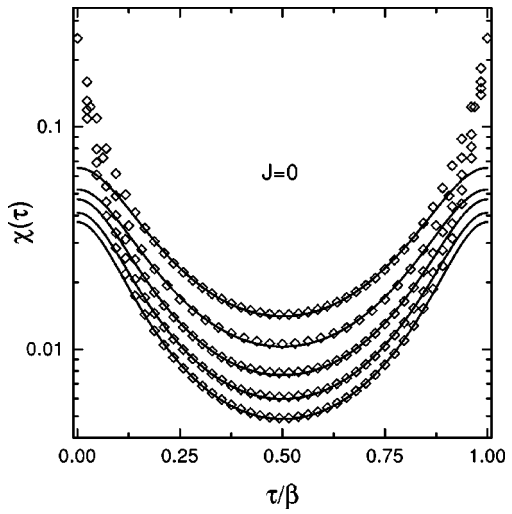

FIG. 1. Dynamic spin susceptibility in imaginary time for $J=0$ for $\beta/\tau_0=18$, 20, 24, 28, and 32, from top to bottom. The symbols are the Monte Carlo data. The solid lines are the fits referred to in the text.

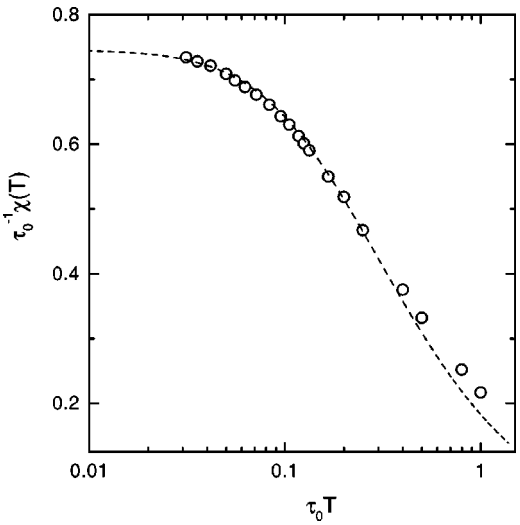

FIG. 2. Temperature dependence of the susceptibility for $J=0$. The circles are the Monte Carlo results. The dashed line represents the susceptibility of the resonant model.

nience. For the particular case $\alpha=1/2$ and for all values of $J_\perp$, the Kondo model is equivalent to a simple exactly solvable problem, the resonant model.[21] We have made this choice as it provides us with means to test our numerical methods by comparison of the Monte Carlo results with the analytical solution. We have taken τ_0^{-1} as the unit of energy and we have arbitrarily set $J_\perp=3/2\tau_0^{-1}$.

Figure 1 shows $\chi(\tau)$ as a function of the scaled variable τ/β for $J=0$ and several temperatures. The correlation function in imaginary time is real and symmetric around $\tau=\beta/2$ as a consequence of time-reversal invariance. Its minimum value steadily decreases with decreasing temperature. The expected behavior of the zero-temperature dynamic susceptibility in the long-time limit is[16] $\chi(\tau)\propto\tau^{-2}$. At finite temperatures this expression generalizes to $\chi(\tau)\sim(\pi/\beta)^2\sin^{-2}(\pi\tau/\beta)$.[22] We have fitted our data for $\tau\sim\beta/2$ with the expression

$$\chi(\tau)=\left(\frac{\pi}{\beta}\right)^2\frac{A}{\sin^2\frac{\pi\tau}{\beta}+\sin^2\frac{\pi\tilde{\tau}}{\beta}}, \tag{17}$$

where A is a T-dependent amplitude and the cutoff $\tilde{\tau}$ is of the order of the inverse of the Kondo temperature to be defined below. The fits, shown by the solid lines in the figure, are in excellent agreement with the numerical data.

The static spin susceptibility has been computed from the Monte Carlo results using the expression[13] $\chi_T=\int_0^\beta d\tau\chi(\tau)$. The results thus obtained are shown in Fig. 2. We also show for comparison the susceptibility of the resonant model,

$$\chi_T=\frac{1}{2\pi^2 T}\phi\left(\frac{1}{2}+\beta\frac{\Delta}{4\pi}\right), \tag{18}$$

where $\phi(z)=d^2\ln\Gamma(z)/dz^2$ and Δ is the width of the resonant level. The latter has been determined by fitting the data for $\tau_0 T\leqslant 0.2$ to Eq. (18) with the result $\Delta=0.827\ \tau_0^{-1}$. There is very good agreement between the theoretical expression and the Monte Carlo results in this temperature range. Deviations from the theoretical result are expected (and observed) at higher temperatures as Eq. (18) is only valid for $T\tau_0\ll 1$. Taking the $T\to 0$ limit of Eq. (18) we find the zero-temperature susceptibility $\chi_0=2/(\pi\Delta)\approx 0.77\ \tau_0$. Defining the Kondo temperature by $\chi_0=1/(2\ T_K^0)$, we obtain $T_K^0\tau_0\approx 0.65$.

We have similarly computed the τ-dependent susceptibility of the system for several values of $J\neq 0$ and T. The overall shape of the curves thus obtained is similar to that of those of Fig. 1 but the decay of the correlations becomes slower and slower as J increases. This is shown in Fig. 3 where we show results obtained for several values of J at our lowest temperature, $T\tau_0=32^{-1}$. This slowing down of the spin dynamics, which is accompanied of an increase of the susceptibility, is a precursor effect of the phase transition that, as we shall see next, takes place for sufficiently large J.

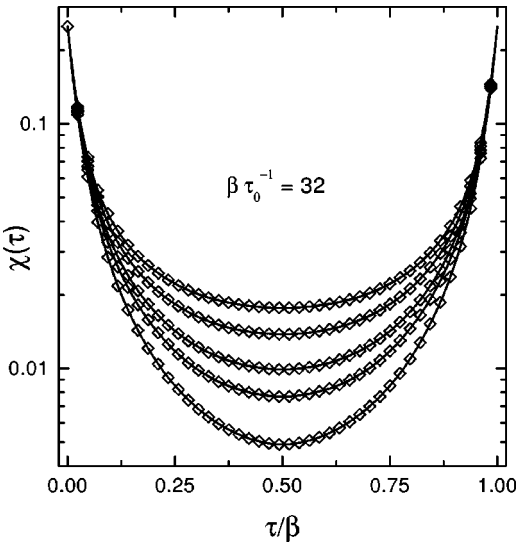

FIG. 3. The J dependence of the dynamic spin susceptibility in imaginary time at fixed temperature, $T\ \tau_0=1/32$. The values of $J\tau_0$ are 0, 0.6, 0.65, 0.7, and 0.75, from bottom to top. The symbols are the Monte Carlo data. The lines are guides for the eye.

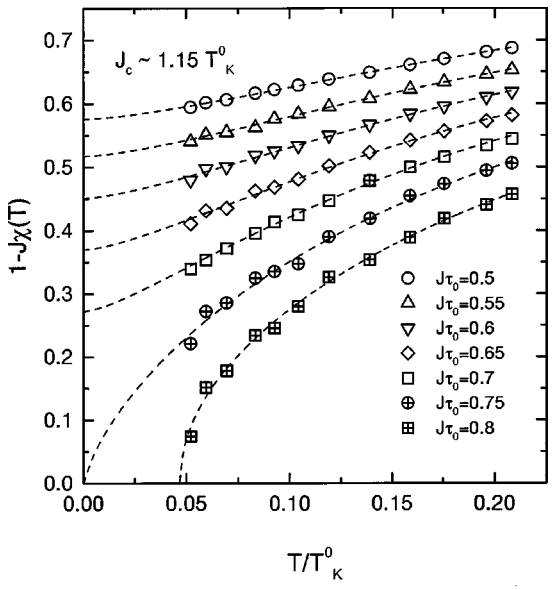

FIG. 4. The J- and T-dependence of $Y(J,T)=1-J\chi_T$. The paramagnetic phase is stable for $Y(J,T)>0$.

A necessary condition for the stability of the paramagnetic phase is that the inequality is $Y(T)\equiv 1-J\chi_T \geqslant 0$ holds.[13] $Y(T)$ is plotted versus temperature in Fig. 4 for several values of J. The symbols are the Monte Carlo data. The dashed lines are fits of the results to a model that will be discussed below and that allows us to extrapolate the results down to $T\rightarrow 0$. We see that $Y(T=0)$ vanishes for $J=0.75\ \tau_0^{-1}\sim 1.15\ T_K^0$, which identifies it as the critical coupling. For $J>J_c$ $Y(T)$ vanishes at a finite temperature, T_g.

Before discussing in detail the temperature dependence of the uniform susceptibility in the vicinity of the critical coupling, we shall make a disgression in order to derive a simple model in terms of which the numerical data can be analyzed in a transparent way. We start by noticing that the frequency-dependent susceptibility may be related to the fluctuations of the auxiliary field $\xi(\tau)$. Using Eqs. (11) and (3) one may readily show that

$$\langle|\xi(i\omega_n)|^2\rangle = Q(i\omega_n)[1+\chi(i\omega_n)Q(i\omega_n)], \tag{19}$$

where the expectation value on the left-hand side of the equation is taken with respect to the probability distribution $\mathcal{P}[\xi(\tau)]\propto\exp(-\beta\mathcal{F})$ with

$$\mathcal{F}[\xi(\tau)] = \mathcal{F}[0] + \frac{kT}{2}\sum_n \frac{|\xi(\omega_n)|^2}{Q(\omega_n)} - kT\ln\left\langle \mathcal{T}\exp\left[\int_0^\beta d\tau\,\xi(\tau)S_z(\tau)\right]\right\rangle_\Gamma . \tag{20}$$

Here, $\beta\mathcal{F}[0]=-\ln[2\cosh(\beta\Gamma/2)]$ and $\langle(\cdots)\rangle_\Gamma = \mathrm{Tr}[(\cdots)\exp(\beta\Gamma S_x)]/\mathrm{Tr}[\exp(\beta\Gamma S_x)]$. Assuming for the moment that the transverse part of the effective field dominates over its fluctuating longitudinal component, $\Gamma \gg \langle\xi^2(\tau)\rangle^{1/2}$, the free-energy (20) may be expanded up to second order in ξ

$$\mathcal{F}[\xi(\tau)] = \mathcal{F}[0] + \frac{kT}{2}\sum_n [Q^{-1}(\omega_n)-\chi^{(0)}(\omega_n)]|\xi(\omega_n)|^2 + \cdots, \tag{21}$$

where the zeroth-order transverse susceptibility $\chi^{(0)}(\omega_n)=\Gamma m_x/(\Gamma^2+\omega_n^2)$ and $m_x=1/2\tanh(\beta\Gamma/2)$. Combining Eqs. (21) and (19) we derive the following expression for the frequency-dependent susceptibility

$$\chi(\omega_n)=\frac{1-\chi^{(0)}(\omega_n)K(\omega_n)-\sqrt{[1-\chi^{(0)}(\omega_n)K(\omega_n)]^2-[2J\chi^{(0)}(\omega_n)]^2}}{2J^2\chi^{(0)}(\omega_n)}, \tag{22}$$

where $K(\omega_n)$ is the Fourier transform of the first term on the right-hand side of Eq. (10). In the limit $T\tau_0,\ |\omega_n|\tau_0 \ll 1$ this is

$$K(\omega_n)=\frac{2\pi\alpha}{\tau_0}(1-|\omega_n|\tau_0+\cdots). \tag{23}$$

Substituting this expansion in Eq. (19) we find

$$\chi(\omega_n)=\frac{1}{J^2}\left\{\frac{\omega_n^2}{\Gamma}+T_K+\tilde{\alpha}|\omega_n| - \sqrt{\left[\frac{\omega_n^2}{\Gamma}+T_K+\tilde{\alpha}|\omega_n|\right]^2-J^2}\right\}, \tag{24}$$

where $\tilde{\alpha}=\pi\alpha$, $T_K=\Gamma-\tilde{\alpha}/\tau_0$ and we have assumed $T\ll\Gamma$. From Eqs. (24) and (19) we can estimate $\langle\xi^2(\tau)\rangle\approx(J^2+2\alpha/\tau_0^2)$ at large Γ. We, therefore, expect Eq. (24) to be valid provided the condition

$$\Gamma\tau_0 \gg \max\{J\tau_0,\sqrt{2\alpha}\}, \tag{25}$$

is satisfied. It is clear that Eq. (25) will not be fulfilled by the bare parameters, in general. We can, however, imagine writing down a set of renormalization-group equations for the flow of the different couplings as the high-energy cutoff is reduced. By analogy with the single-impurity case, we expect that in the paramagnetic phase the Kondo couplings will flow to the strong-coupling fixed-point $\Gamma\equiv J_\perp^K\rightarrow\infty$. Therefore, we expect Eq. (24) to become appropriate below some energy scale with renormalized values of the couplings.

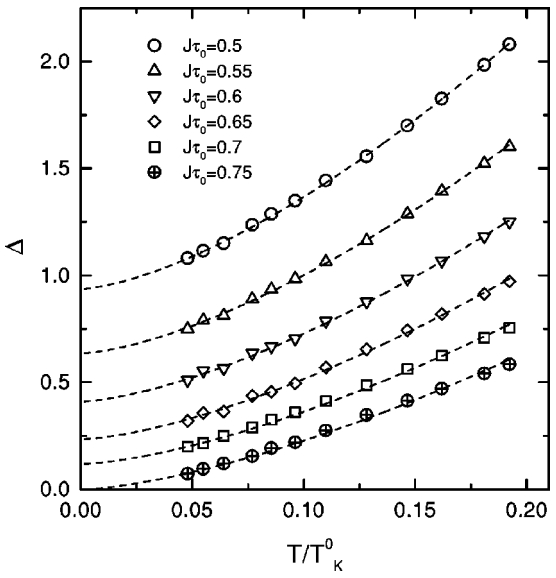

FIG. 5. The J and T dependence of Δ. The symbols are the Monte Carlo data. The dashed lines are the fits to the expression in Eq. (28).

The derivation of the renormalization-group equations for the Kondo-alloy model is outside the scope of this work.[23] We shall instead consider Eq. (24) as a phenomenological equation containing three renormalized parameters, T_K, $\tilde{\alpha}$, and Γ to be determined by a fit of the numerical results.

The ratio T_K/J is determined by the static uniform susceptibility alone. Setting $\omega_n=0$ in Eq. (24) we have

$$J\chi_T=\frac{T_K}{J}-\sqrt{\frac{T_K^2}{J^2}-1}. \tag{26}$$

We thus see that the instability of the paramagnetic phase is signaled by the vanishing of the quantity under the square root in Eq. (26). We may therefore take $\Delta=T_K^2/J^2-1$ as a measure of the distance to the quantum-critical point and rewrite the susceptibility in the form

$$J\chi_T=\sqrt{1+\Delta}-\sqrt{\Delta}. \tag{27}$$

Notice that, even if the assumptions made in the derivation of Eq. (27) are not valid, the latter can still be regarded as a parametrization of the susceptibility in terms of a new quantity, $\Delta(T,J)$. The interest of this parametrization stems from the fact that the T- and J-dependence of Δ is very simple. We show in Fig. 5 the numerical values of Δ obtained inserting the Monte Carlo results for the static susceptibility in Eq. (27). The dashed lines are fits to the simple functional form

$$\Delta(T)=\Delta_0+(T/T_0)^{3/2}, \tag{28}$$

where the parameters Δ_0 and T_0 are functions of J but not of T. The fits are very accurate over the entire temperature range of our simulations. The lowest curve, corresponding to our estimated value for the critical coupling, has been fitted with $\Delta_0=0$. Examination of the J dependence of Δ_0 shows that, near J_c, $\Delta_0\to a(1-J/J_c)$, with $a\approx 1$. The parameter T_0 has a finite limit, $T_0\approx 0.27\ T_K^0$ as $J\to J_c$.

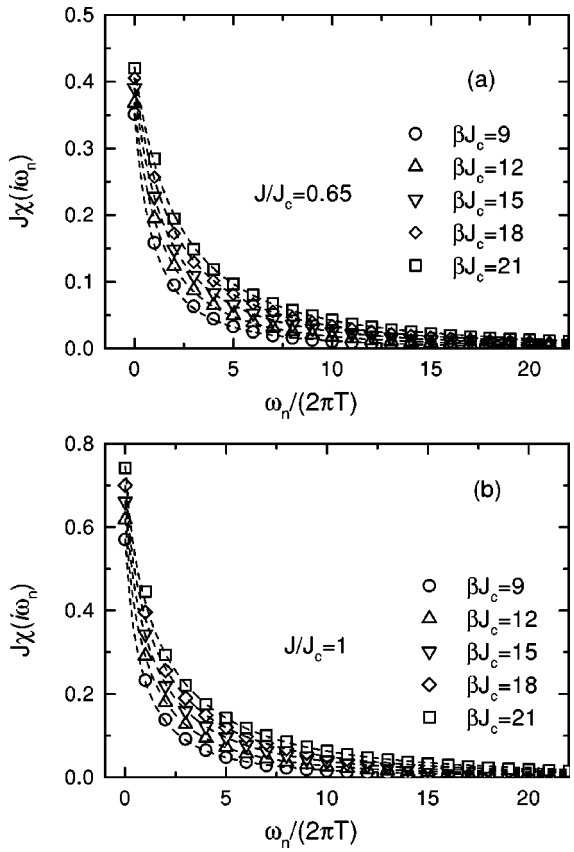

FIG. 6. The ω and T dependence of the dynamic susceptibility for two values of the coupling J. The symbols are the Monte Carlo data. The lines are fits to the expression in Eq. (24).

Equations (27) and (28) imply that, in the neighborhood of the critical coupling, the uniform susceptibility has a non-Fermi-liquid T dependence

$$J_c\chi_T\approx\begin{cases}1-\left(\dfrac{T}{T_0}\right)^{3/4} & \text{for} \quad \Delta_0^{2/3}\ll T/T_0\ll 1,\\[2ex] 1-\sqrt{\Delta_0}-\dfrac{1}{2\sqrt{\Delta 0}}\left(\dfrac{T}{T_0}\right)^{3/2} & \text{for} \quad T/T_0\ll\Delta_0^{2/3}.\end{cases} \tag{29}$$

The values of the exponent γ found in the two regions defined above correspond to those obtained by other authors[4–6] in the quantum critical and quantum disordered I (QDI) regions in their analysis of metallic spin-glass models. A third region (QDII) should exist at lower temperatures where the normal Fermi-liquid T^2 behavior is recovered. This second crossover is not visible in our data because, as we shall see, it occurs below the lowest temperature that we can reach in our quantum Monte Carlo simulations.

The remaining two parameters in Eq. (24) may be determined from an analysis of the full ω_n and T dependence of the susceptibility. This is shown in Fig. 6 for two couplings, $J=0.65\ J_c$ and $J=J_c$. The symbols are the quantum Monte Carlo data. The dashed lines are plots of Eq. (24) with Γ, $\tilde{\alpha}$ and T_K adjusted to fit the data. The quality of the fits is excellent for all the values J and T considered. It is remarkable that *all* our numerical results could be fitted with the

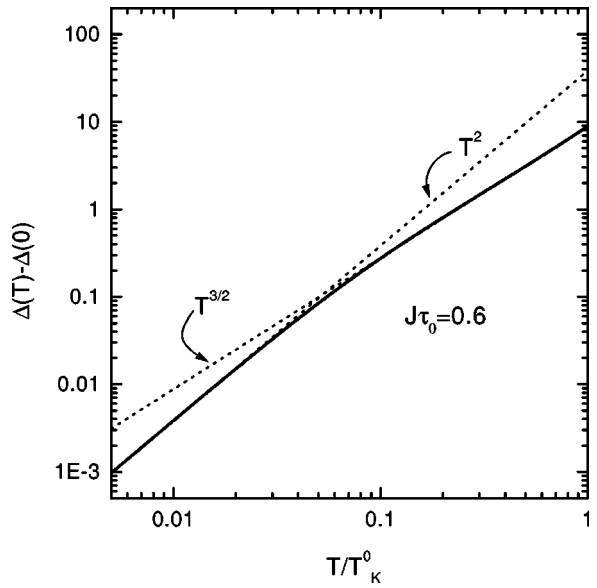

FIG. 7. The crossover between anomalous and Fermi-liquid behavior obtained from Eq. (24) and condition (31).

same values of $\Gamma\tau_0 \approx 2.4$ and $\tilde{\alpha} \approx 1.48$. The full J- and T-dependence is therefore in the effective Kondo temperature, T_K. The values of T_K obtained from the fits of the frequency dependence of the susceptibility are consistent with those determined above from the static susceptibility.

At this point, we can discuss the connection between our results and those of Sengupta and Georges.[5] Phrased in our language, their approximation for $\chi(\omega_n)$ is obtained by ignoring the transverse field term in Eq. (11), and solving the remaining Ising problem in the spherical approximation. The expression for the dynamic susceptibility that results from this procedure is

$$\chi(\omega_n) \approx \frac{1}{J^2}\{\lambda + \tilde{\alpha}|\omega_n| - \sqrt{[\lambda+\tilde{\alpha}|\omega_n|]^2 - J^2}\}, \quad (30)$$

where λ is a Lagrange multiplier introduced to impose the spherical constraint,

$$\langle S_z(\tau) S_z(\tau)\rangle = \frac{1}{\beta}\sum_{n=-\infty}^{\infty} \chi(\omega_n) = 1/4. \quad (31)$$

As it stands, expression (31) diverges because Eq. (30) does not have the correct ω_n^{-2} high-frequency behavior. A high-energy cutoff Λ must therefore be introduced in the simplified model.

Comparison of Eqs. (24) and (30) shows that the two expressions become equivalent at low frequencies provided we identify T_K with λ and $\tilde{\alpha}\Gamma$ with Λ. The fact that the Monte Carlo data could be fitted using Eq. (24) with T- and J-independent values of $\tilde{\alpha}$ and Γ justifies *a posteriori* the use of a constant cutoff in the simplified model. Once this is fixed, the parameter λ can be determined from condition (31). Since the numerical data do satisfy this normalization, it is not surprising that the determination of T_K from fits of the Monte Carlo data and that of λ from enforcement of Eq. (31) result in the same temperature dependence. This suggests that Eq. (24) may be used in conjunction with the normalization condition to estimate the T dependence of Δ in the temperature range where we do not possess numerical data. We show in Fig. 7 the result of applying this procedure to the case of $J=0.8\ J_c$. We see that the expected crossover from a $T^{3/2}$ law to normal T^2 behavior occurs at a temperature $T^\star \approx 0.06\ T_K^0$. This is at the lower end of the temperature range that we can reach. The crossover temperature further diminishes as $J \to J_c$ where it vanishes. This explains why normal behavior has not been seen in our simulations.

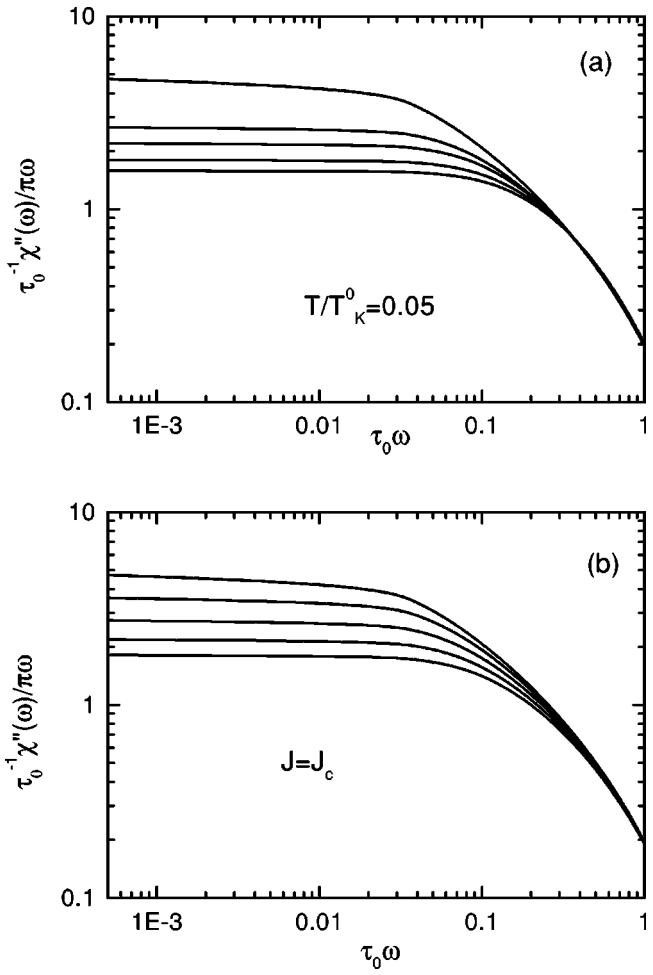

FIG. 8. The relaxation function, $\chi''(\omega)/\omega$. The curves have been obtained by analytic continuation of the fits of the imaginary-time Monte Carlo data. (a) $T/T_K=0.05$ and $J\tau_0=0.55$, 0.6, 0.65, 0.7, and 0.75, from top to bottom. (b) $J=J_c$ and $\beta/\tau_0=32$, 28, 24, 20, and 16, from top to bottom.

The imaginary part of the magnetic response can now be determined by analytic continuation of Eq. (24). The general expression is complicated and not very illuminating. However, in the low-frequency limit, $\omega \ll \tilde{\alpha}\Gamma$, and for $J \to J_c$, Eq. (24) can be cast in the scaling form

$$J_c\chi''(\omega) = \sqrt{\Delta}\,\Phi\left(\frac{2\tilde{\alpha}\omega}{J_c\Delta}\right), \quad (32)$$

where the universal scaling function $\Phi(x)$

$$\Phi(x) = \frac{1}{\sqrt{2}} x[(1+x^2)^{1/2}+1]^{-1/2}. \quad (33)$$

This expression is equivalent to that found in Refs. 4–6.

The low-frequency behavior of $\chi''(\omega)$ as $J \to J_c$ follows from the above equations

$$J_c \chi''(\omega) \approx \begin{cases} \dfrac{\tilde{\alpha}\omega}{J_c \Delta} & \text{for} \quad \omega \ll J_c \Delta, \\ \left(\dfrac{\tilde{\alpha}\omega}{J_c} \right)^{1/2} & \text{for} \quad J_c \Delta \ll \omega \ll \tilde{\alpha}\Gamma. \end{cases} \tag{34}$$

The dissipative part of the susceptibility in the limit $\omega \to 0$ is Fermi-liquid-like everywhere except at the quantum-critical point. However, the characteristic spin-fluctuation frequency $\omega_{sf} \propto J_c \Delta$ vanishes as $J \to J_c$ with $\omega_{sf} \propto (1 - J/J_c)$ for $J \lesssim J_c$ and $\omega_{sf} \propto T^{3/2}$ at the critical coupling. The behavior of $\chi''(\omega)$ at J_c is non-Fermi-liquid-like, $\chi''(\omega) \propto \sqrt{\omega}$, which reflects the slow decay of the time-dependent spin-spin correlation function, $\langle S_z(t) S_z(0) \rangle \sim t^{-3/2}$ that anticipates the appearence of long-range order in the system. The nontrivial T-dependence of the spin-fluctuation frequency in the vicinity of the quantum-critical point that is responsible for the singular behavior of the susceptibility gives rise to anomalous powers in other thermodynamic and transport properties as well. In particular, Eqs. (32) and (33) imply that the temperature corrections to the specific heat and the resistivity behave, respectively, as $\delta C/T \propto -\sqrt{T}$ and $\delta\rho \propto T^{3/2}$, in the quantum-critical region.[4,5]

The full ω-dependence of the absorptive part of the dynamic susceptibility is shown in Fig. 8 for several temperatures at the critical coupling and several values of J at $T = 0.05\ T_K^0$. These curves have been computed by analytically continuing the fits of the imaginary-frequency Monte Carlo data. These curves are very similar in shape to those obtained in Ref. 20 for the single-impurity Kondo model and may be characterized by an effective Kondo temperature that decreases with the distance to the quantum-critical point where it vanishes. Indeed, Eqs. (32) and (33) imply that the effective Kondo scale ω_K, defined as the half width of the relaxation function $\chi''(\omega)/\omega$, is $\omega_K \sim T_K^{(0)} \sqrt{\Delta}$.

V. CONCLUSIONS

In this paper, we have studied numerically a Kondo lattice model with random exchange between localized spins. A mapping of this model to a self-consistent single-spin problem, exact in the limit of large lattice coordination, allowed us to obtain a complete numerical solution of the problem. The system has a quantum-critical point between a normal metal and a spin-glass state. There is a region in the $T-J$ plane near the quantum-critical point where the characteristic spin-fluctuation energy varies as a nontrivial power of temperature ($\omega_{sf} \propto T^{3/2}$). This gives rise to non-Fermi-liquid behavior in thermodynamic and transport properties. At low-enough temperature normal Fermi liquid behavior is recovered, except at the critical coupling. Our numerical results can be very well described over a large range of frequency and temperature by a simple model that we derive in the strong-coupling limit. This model is closely related to the M-component quantum-rotor and mean-field models that have been previously discussed in the literature.[4–6] Some interesting questions remain open, notably, to what extent the assumption that the electronic bath remains unrenormalized is a valid one. The enforcement of the self-consistency condition (4) poses some important technical difficulties, which we hope to be able to overcome in future work.

ACKNOWLEDGMENTS

One of us (M. J. R.) acknowledges the support of Fundación Antorchas, CONICET (PID No. 4547/96), and ANPCYT (PMT-PICT1855).

*Present address: Service de Physique de l'Etat Condensé, CEA-Saclay, 91191 Gif-sur-Yvette, France.

[1] See, for instance, *Conference on Non-Fermi Liquid Behavior in Metals* [J. Phys.: Condens. Matter **8** (1996)].
[2] M. B. Maple *et al.*, J. Low Temp. Phys. **99**, 223 (1995).
[3] E. Miranda, V. Dobrosavljević, and G. Kotliar, Phys. Rev. Lett. **78**, 290 (1997).
[4] S. Sachdev, N. Read, and R. Oppermann, Phys. Rev. B **52**, 10 286 (1995).
[5] A. M. Sengupta and A. Georges, Phys. Rev. B **52**, 10 295 (1995).
[6] S. Sachdev, Philos. Trans. R. Soc. London, Ser. A **356**, 173 (1998).
[7] A. J. Millis, Phys. Rev. B **48**, 7183 (1993).
[8] N. Read, S. Sachdev, and J. Ye, Phys. Rev. B **52**, 384 (1995).
[9] W. Metzner and D. Volhardt, Phys. Rev. Lett. **62**, 324 (1989).
[10] D. Sherrington and S. Kirkpatrick, Phys. Rev. Lett. **35**, 1792 (1975).
[11] J. A. Hertz, Phys. Rev. B **14**, 1165 (1976).
[12] A. Georges, G. Kotliar, W. Krauth, and M. J. Rozenberg, Rev. Mod. Phys. **68**, 13 (1996).
[13] A. J. Bray and M. A. Moore, J. Phys. C **13**, L655 (1980).
[14] A. Georges and G. Kotliar, Phys. Rev. B **45**, 6479 (1992).
[15] D. R. Grempel and M. J. Rozenberg, Phys. Rev. Lett. **80**, 389 (1998).
[16] P. W. Anderson, G. Yuval, and D. R. Hammann, Phys. Rev. B **1**, 4464 (1970).
[17] Qimiao Si and G. Kotliar, Phys. Rev. Lett. **70**, 3143 (1993); Phys. Rev. B **48**, 13 881 (1993).
[18] M. J. Rozenberg and D. R. Grempel, Phys. Rev. Lett. **81**, 2550 (1998).
[19] P. W. Anderson and G. Yuval, J. Phys. C **4**, 607 (1971).
[20] S. Chakravarty and J. Rudnick, Phys. Rev. Lett. **75**, 501 (1995).
[21] F. Guinea, V. Hakim, and A. Muramatsu, Phys. Rev. B **32**, 4410 (1985).
[22] G. Yuval and P. W. Anderson, Phys. Rev. B **1**, 1522 (1970).
[23] A qualitative description of the renormalization group flows in the vicinity of the quantum transition has been given for the case of a related model by Q. Si and J. Lleweilun Smith, Phys. Rev. Lett. **16**, 3391 (1996).